Lat. Am. J. Aquat. Res., 44(2): 293-304, 2016
DOI: 10.3856/vol44-issue2-fulltext-10

Research Article

Analysis of flood pulse dynamics in the lower basin of the San Pedro River (northwestern Mexico) using remote sensing

Rafael Hernández-Guzmán[1], Arturo Ruiz-Luna[2], César A. Berlanga-Robles[2] & Jesús T. Ponce-Palafox[3]
[1]CONACYT Research Fellow, Instituto de Investigaciones sobre los Recursos Naturales
Universidad Michoacana de San Nicolás de Hidalgo, C.P. 58330, Morelia, Michoacán, México
[2]Centro de Investigación en Alimentación y Desarrollo A.C., Coordinación Regional Mazatlán
Mazatlán, C.P. 82100, Sinaloa, México
[3]Centro Multidisciplinario de Bahía de Banderas, Escuela Nacional de Ingeniería Pesquera
Laboratorio Bioingeniería Costera, Universidad Autónoma de Nayarit
Tepic, C.P. 63155, Nayarit, México
Corresponding autor: Arturo Ruiz Luna (arluna@ciad.mx)

ABSTRACT. This paper analyzes inter-annual (1993-2008) and intra-annual (2006-2008) flooding patterns in the unregulated San Pedro River, based on digital analysis of two Landsat satellite imagery series and ancillary rainfall and discharge data, to describe variations in the natural pulse. The long-term pattern, over a period of 16 years, showed considerable fluctuations, with a maximum flood extent (FE) of approximately 200 km^2, while the observed average was 57.8 km^2 over the entire period, around 24 km^2 the dry season and more than 90 km^2 in the rainy season. The seasonal variation, analy zed using 29 quasi-monthly images recorded from 2006 to 2008, displayed FE peaks in the rainy season (July to October) with variations in time and extent that were not directly related to rainfall but instead were related to river discharge, Q, ($FE = y_0 + a(1\text{-}0.9983^{Q})$; $R^2 = 0.91$). We used the above exponential model with monthly average river discharge data (1944-2008) and the proposed regulated volume of discharge from governmental plans to construct a dam on the San Pedro River. We found that the natural ecosystem will be altered by increasing the inundation in the dry season and reducing it in the rainy season. This change will have consequences in coastal wetlands and aquatic biota adapted to historical conditions, with consequences for the production of aquatic organisms and for ecosystem services.

Keywords: hydrologic pulse, flooding, coastal wetlands, modeling, northwestern Mexico.

Análisis de la dinámica de pulsos de inundación de la cuenca baja del Río San Pedro (México noroccidental) mediante teledetección

RESUMEN. De acuerdo al análisis digital de dos series temporales de imágenes del satélite Landsat y datos de precipitación y flujo, se analizaron los patrones de inundación inter-anual (1993-2008) e intra-anual (2006-2008) del Río San Pedro, para describir variaciones en su pulso natural. En largo plazo (16 años), se detectaron amplias fluctuaciones con una superficie máxima de inundación (FE) cercana a 200 km^2 y una extensión media anual de 57,8 km^2, con promedios aproximados de 24 y 90 km^2 para las temporadas seca y lluviosa, respectivamente. La variación intra-anual, evaluada a partir de 29 imágenes, registradas con periodicidad cuasi-mensual en el periodo 2006-2008, mostró máximos de FE en la temporada lluviosa (julio a octubre), con diferencias en tiempo y espacio, no relacionadas directamente con la precipitación, sino asociadas con el escurrimiento (Q) del río, ($FE = y_0 + a(1\text{-}0{,}9983^{Q})$; $R^2 = 0{,}91$). Este modelo exponencial se aplicó a una serie temporal con datos promedio mensuales de escurrimiento (1944-2008) y con los volúmenes de descarga regulada propuestos para el plan de construcción de una presa en el Río San Pedro. Se concluye que los ecosistemas naturales serán alterados con un aumento de la superficie inundada durante la época de sequía y una reducción en la época de lluvia. Este cambio tendrá consecuencias sobre los humedales costeros y la biota acuática adaptada a condiciones desarrolladas históricamente, con consecuencias para la producción de organismos acuáticos y para los servicios ecosistémicos.

Palabras clave: pulso hidrológico, inundación, humedales costeros, modelación, México noroccidental.

Corresponding editor: Nelson Silva

INTRODUCTION

The variability of seasonal and inter-annual extent, timing and magnitude of inundation of floodplains, frequently described as flood pulse (Junk *et al.*, 1989), is currently recognized as an important driver for more resilient floodplains, maintenance of biodiversity, biomass production and decomposition (Middleton, 2002) beyond the simple exchange of organic matter and solids between the main channel and the floodplain (Benke *et al.,* 2000). Therefore, constancy of flood pulses is related to biota well adapted to changes in water levels, allowing it to efficiently use habitat and resources throughout time (Junk *et al.,* 1989; Junk & Wantzen, 2004). Additionally, changes in flood patterns are seen as responsible for alterations in the functional dynamics of wetlands, and thus on their maintenance, carbon exchange, productivity and ecosystem services delivery. Those changes frequently happen in relation to regional development, hydraulic infrastructure development (dams, reservoirs, channels, and ponds) occurring for agriculture, aquaculture, energy production and urban purposes.

The flood pulse and all its effects cannot be fully understood without quantification of its most essential component: its inundation dynamics. Inundation dynamics can be defined as the temporal and spatial pattern of floodplain inundation, which usually occurs and vary at inter-annual scale. Inundation dynamics are dependent on both discharge dynamics and the delineation of floodplain areas, both of which have been described in detail for many river systems (*e.g.,* Benke *et al.,* 2000).

Consequently, understanding of the variability of annual floods has become an essential input for wetland maintenance and rehabilitation, requiring information on seasonal and inter-annual flooding patterns (Infante-Mata *et al.,* 2012; Rebelo *et al.,* 2012). Because flooding fluctuations may affect the biota in different ways, it is important to evaluate its dynamics for further analysis regarding their effects on the ecosystems. However, observations to evaluate flooding variability are limited in space and time. Therefore remote sensing (RS) applications become a useful tool for assessing inundated floodplains in barely accessible ecosystems, by providing consistent and systematic observations from the Earth's surface. However, RS has technical limitations when delineating those transitional environments, particularly for low- to medium-resolution imagery (Townshend & Justice, 1990) and when wetland vegetation mosaics have a patchy distribution, or have small, isolated or diffuse patterns (Knight *et al.,* 2009).

To overcome the technical limitations of RS, synthetic aperture radar (SAR) is currently used (Matgen *et al.,* 2006; Martinez & Le Toan, 2007; Rebelo *et al.,* 2012). However, the cost and availability of SAR data cannot compete yet with optical multispectral imagery, which additionally integrates the largest time series for landscape change analysis (Frazier & Page, 2009; Qi *et al.,* 2009; Chormanski *et al.,* 2011; Pricope, 2012). Considering this, we used a combination of historical imagery from Landsat TM and ETM+ sensors (1993-2008) to assess and document seasonal patterns and inter-annual variability of flooding extent in the lower basin of the San Pedro River, which is one of the main streams that supplies Marismas Nacionales, the largest wetland complex on the Mexican Pacific coast. This complex system is nourished by other rivers besides the San Pedro River, some of them free of dams or other obstacles to flow. The San Pedro River is one of the most important because of its length and volume (Blanco & Correa, 2011; De la Lanza-Espino *et al.,* 2012), but considering the plans to construct a hydroelectric dam in the short term, its functions and ecosystem services delivery are in risk.

We analyzed variations in annual patterns, based on the largest Landsat TM imagery time series available up to 2008, when a large flood was recorded in the study area. We also analyzed a monthly time series for recent years (2006-2008). This series provide historical information on inter- and intra-annual flood pulse variations, helpful for wetlands conservation purposes, flood control and risk prevention, and offers a baseline for future studies or management plans.

Although flood dynamics and duration cannot be followed continuously in time with Landsat imagery, with a snapshot every 16 days, data provided by this satellite program has the largest imagery record, starting from 1973. However, we used images with similar technical characteristics, particularly spatial (30 m pixel) and spectral resolution. This makes the images comparable, reducing uncertainty on the assessed coverages due to image pre-processing and manipulation to fit the scenes to the same pixel sizes and geographic position, being possible to detect small water ecosystems (>0.01 km^2), which is important for documenting changes occurring in relatively short periods, which is required to estimate flood pulses with the precision desirable for the purposes of this study.

With those considerations, but having in mind that more information is better for an effective environmental management, this study proposes a low cost approach to analyze the inter and intra-annual flooding patterns of the unregulated San Pedro River floodplain

and analogous systems, required to prevent or mitigate negative impacts from natural events or human actions.

MATERIALS AND METHODS

The study area is part of Marismas Nacionales (MN), a large and complex ecosystem located in northwest Mexico, between Sinaloa and Nayarit states. It integrates different types of coastal wetlands, highlighting lagoons, saltmarsh, and mangroves. The mangrove forests are among the largest and most developed in the eastern Pacific, covering approximately 750 km^2. MN is designated Wetland of International Importance (Ramsar site number 732) and Biosphere Reserve within the system of Natural Protected Areas of Mexico.

From north to south, the rivers Baluarte, Cañas, Acaponeta, Rosamorada, Bejuco, San Pedro and Santiago contribute to the MN system, with the San Pedro River as one of the most important because of its discharge and dam free status. It flows to the ocean, through lacustrine deltas in coastal marshes and lagoons, contributing with suspended solids and sediment to improve habitat and ecological productivity (Ortiz & Pérez, 1999; Blanco & Correa *et al.,* 2011). The lower basin was chosen as the study area for this analysis, with an extent about 580 km^2, defined by the drainage basin limits to the north and south, while western and eastern boundaries match the coastline and the elevation of 10 m above sea level (m.a.s.l.), respectively (Fig. 1).

Agriculture (mostly extensive) covers approximately 50% of the study area, while mangrove (approximately 15%) together with other wetlands (lagoons, saltmarsh) amount to 25% of the area (Hernández-Guzmán *et al.*, 2008). The San Pedro River discharges 2740 million cubic meters per year on average (measured at the San Pedro gauging station), with an estimated laminar flow of approximately 106 mm and runoff coefficient of 7.9%, which are consistent with forested or agriculture covers (INEGI, 1999; Hernández-Guzmán *et al.,* 2008).

The mean annual temperature ranges from 14 to 26°C, while rainfall varies from 700 to 2000 mm per year. The highest rainfall rates occur in the rainy season, from June to October, and down to the minimum in the dry season (November-May). The flooding pulse is seasonally marked close to the river mouth, and it is influenced by the tidal regime that displays curves with mixed semi-diurnal, low amplitude tides (maximum peak 1.1 m). The mean tide reaches around 0.7 m, and maximum spring tides occur on June and December while minimum neap tides are present during March and September (Stillman & Barnwell, 2004; Valdez, 2004). In this area, diverse estuaries, ponds and lagoons integrate to form a complex system, with Laguna Grande de Mexcaltitan, Estero Grande, Las Gallinas, Macho, El Tanque and El Mezcal as the most notable water bodies (INEGI, 1999).

To assess the inter- and intra-annual flood extent and flooding pulse dynamics in the lower San Pedro River watershed, satellite imagery from the Landsat TM and ETM+ sensors, recorded every 16 days over the study area, was used. Images boundaries are defined by the path-row 30-45 or 31-45 of the world reference system WRS2. The scenes, covering above 30,000 km^2 each, were selected for both, dry and rainy seasons, depending on their quality, that could be affected by weather conditions. The imagery was downloaded from the Earth Resources Observation and Science Center (EROS) of the U.S. Geological Survey (USGS), through the Global Visualization viewer (http://glovis.usgs.gov).

The largest, continuous, image time series was used for the inter-annual FE analysis, while only the last three years of the study period (2006 to 2008) were included for the intra-annual analysis, limited by the available hydrologic data and considering a high runoff peak detected in 2008.

All the scenes fit the same spatial resolution (30 m pixel), geographic boundaries and projection (UTM 13N; NAD83) and were subsequently classified using the K-means unsupervised classification technique, which splits an n-dimensional imagery into K exclusive clusters, assigning each pixel to the cluster whose centroid is nearest (Richards & Jia, 1999). With exception of the Landsat thermal band 6, all the spectral bands were used in the classification process.

This produced at least 30 spectral classes per scene, which were aggregated into flood extent (FE) and a second class (Land) including all those different from water, producing binary water/land maps (1 = water; 0 = land). Because spectral signatures for water are rarely confused with other land cover types, decreasing reflectance from the visible blue to the near infrared in the Landsat bands, and regarding that Berlanga-Robles & Ruiz-Luna (2006, 2011) and Berlanga-Robles *et al.* (2008) suggest that accuracy of the classification is overestimated when aquatic surface was included in the assessment, the accuracy for flood extent was not assessed. When clouds were present (<7% in the worst case), their interference with water detection was overcome by analyzing the closest dated scenes. The results were then added to the final map by date.

Finally, the estimated FE (km^2) series was analyzed to detect possible relationships with rainfall R (mm) and monthly river discharge Q (10^6 m^3). Data were recor-

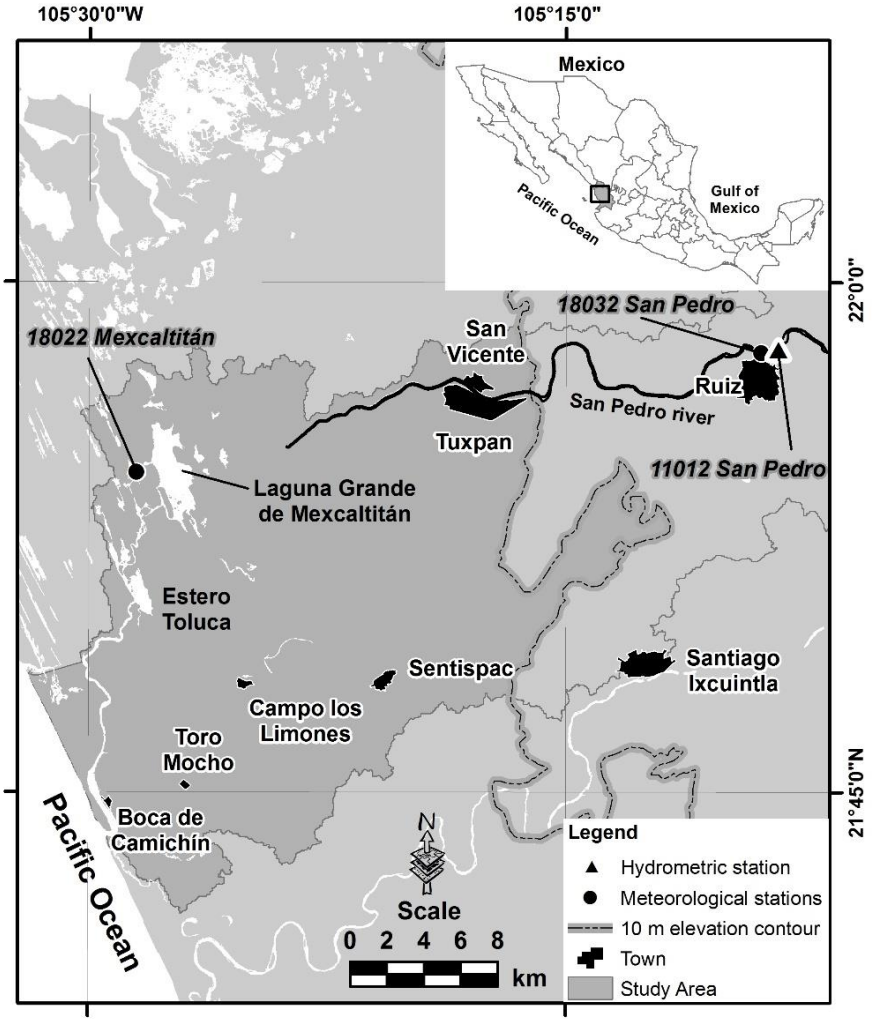

Figure 1. Geographic location of the study area in Nayarit State, Mexico, displaying main urban localities and water bodies.

ded daily in the study area (San Pedro 11012 hydrometric station and meteorological stations Mexcaltitan 18022 and San Pedro 18032, separated by a distance of 35 km), and are provided in monthly report format by the National Water Council (CONAGUA by its Spanish acronym). Previous studies on flood extent suggest that data can be fitted to linear or non-linear models to explain flooding, based on the discharge patterns and river characteristics (Smith *et al.,* 1995; Benke *et al.,* 2000; Frazier *et al.,* 2003). Here, we used both linear and non-linear regression models to explain possible patterns in the flooding process in the lower San Pedro River watershed. This method is informative for management purposes and developing strategies to reduce flooding risks. All the statistical analyses were performed using Microsoft Excel 2010 and SigmaPlot 12.0 (Systat Software Inc.).

RESULTS

The Landsat imagery available for the inter-annual analysis include 28 images, selected for the dry (14 scenes) and the rainy seasons (14 scenes), excluding 2003 and 2004 due to the lack of images (Table 1). Regarding the intra-annual assessment, due the weather conditions, only 29 quasi-monthly images were selected for 2006 (10), 2007 (8) and 2008 (11).

Inter-annual flooding patterns

Estimations on flood extent (FE) for dry and rainy seasons did not show a defined flooding pattern and displayed maximum and minimum values during different months along the time series (Table 1). Just considering values estimated for the rainy season by year, the largest FE was detected for the image recorded

Table 1. Inter-annual variation of flood extent in the San Pedro River floodplains (1993-2008), dry and rainy seasons, from satellite data analysis. Dates are for Landsat imagery recording. Light and dark grey are for the minimum and maximum extent along the time series, respectively.

Year	Dry season		Rainy season		Max/Min ratio
	Area (km^2)	Date	Area (km^2)	Date	
1993	27.5	Mar-13	196.1	Sep-14	7.1
1994	30.5	Apr-17	126.9	Oct-19	4.2
1995	30.6	Apr-20	66.2	Jul-09	2.2
1996	20.3	Apr-22	55.7	Oct-15	2.7
1997	24.0	Mar-08	58.9	Sept-16	2.5
1998	26.2	May-13	60.2	Jul-10	2.3
1999	21.2	Mar-30	111.2	Jul-12	5.2
2000	22.8	Apr-17	67.6	Aug-23	3.0
2001	22.4	Mar-19	70.1	Jul-17	3.1
2002	21.0	Jan-09	65.8	Aug-21	3.1
2003	-	-	-	-	-
2004	-	-	-	-	-
2005	21.5	May-01	88.3	Jul-29	4.1
2006	18.4	Apr-02	120.0	Sep-18	6.5
2007	22.8	Apr-14	79.9	Aug-11	3.5
2008	21.0	Mar-22	120.7	Aug-22	5.7
Mean	23.6		92.0		3.8

in September 1993 (196 km^2), but for the same month in 1996, the flood extent displayed the lowest value (55.7 km^2).

Values above the rainy season average (around 92 km^2) were detected at least once for every month in the rainy season, including July when the rainy season starts. July was also the best-represented month in the image series (five dates), with FE ranging from 60.2 to 111.2 km^2. Concerning the dry season, the FE average extent was around 23.6 km^2, basically representing the perennial lagoon surface and its connection with the sea. In this case, April 2006 represented the lowest flood area (18.4 km^2), while the maximum was observed in April 1995 at 30.6 km^2 with a coefficient of variation (CV) lower than 16%, compared with a CV > 40% for the rainy season.

The ratio between the rainy season flood extents (FE_r) against the dry season values (FE_d), varied from 2.2 in July 1995 up to 7.1 in September 1993. This suggests that FE_r are roughly three to four times greater than FE_d, except 1993 when this ratio increased to its maximum value (Fig. 2).

Near to the average flood extent for dry and rainy seasons is also illustrated in Figure 2, displaying satellite scenes recorded in year 2008 (Fig. 2a) and 1996 (Fig. 2b), respectively. High inundation records, as those observed in 1993, 1999, 2006 and 2008, occupy around a fifth up to a third of the study area, particularly to the north where Tuxpan, San Vicente and other small settlements are sited, with population around 30,000 inhabitants. This process totally connects the river with coastal wetlands, except for some small tributaries and isolated areas, with locals taking advantage episodically on soil water retention for agriculture purposes.

Intra-annual flooding variation

Based on rainfall data (R) analysis, the total annual rainfall was almost the same for 2006 and 2007, with approximately 890 mm per year, doubling this figure to 1867 mm in 2008, even though the number of months with rainfall records was the same every year (5). This is due to variation in the rainfall peak and monthly rainfall distribution, including a record in January 2007, which was not observed in the other years included in the analysis (Fig. 3).

The relationship between rainfall (R) and river discharge (Q), when all the monthly values were used, displayed a positive correlation ($r = 0.75$; $P < 0.01$). But when daily data (2006-2008) were assessed, positive correlation coefficient values were lower in both cases, by meteorological station ($r = 0.24$ and 0.26; $P < 0.01$) or using cumulative values ($r = 0.30$; $P < 0.01$). The weakness of this relationship was evident when total Q_{2007} was 18% and 72% lower compared with Q_{2006} and Q_{2008}, even when cumulative rainfall for 2006 and 2007 was practically the same. Changes in temporal rainfall distribution could affect the runoff rates in such a way,

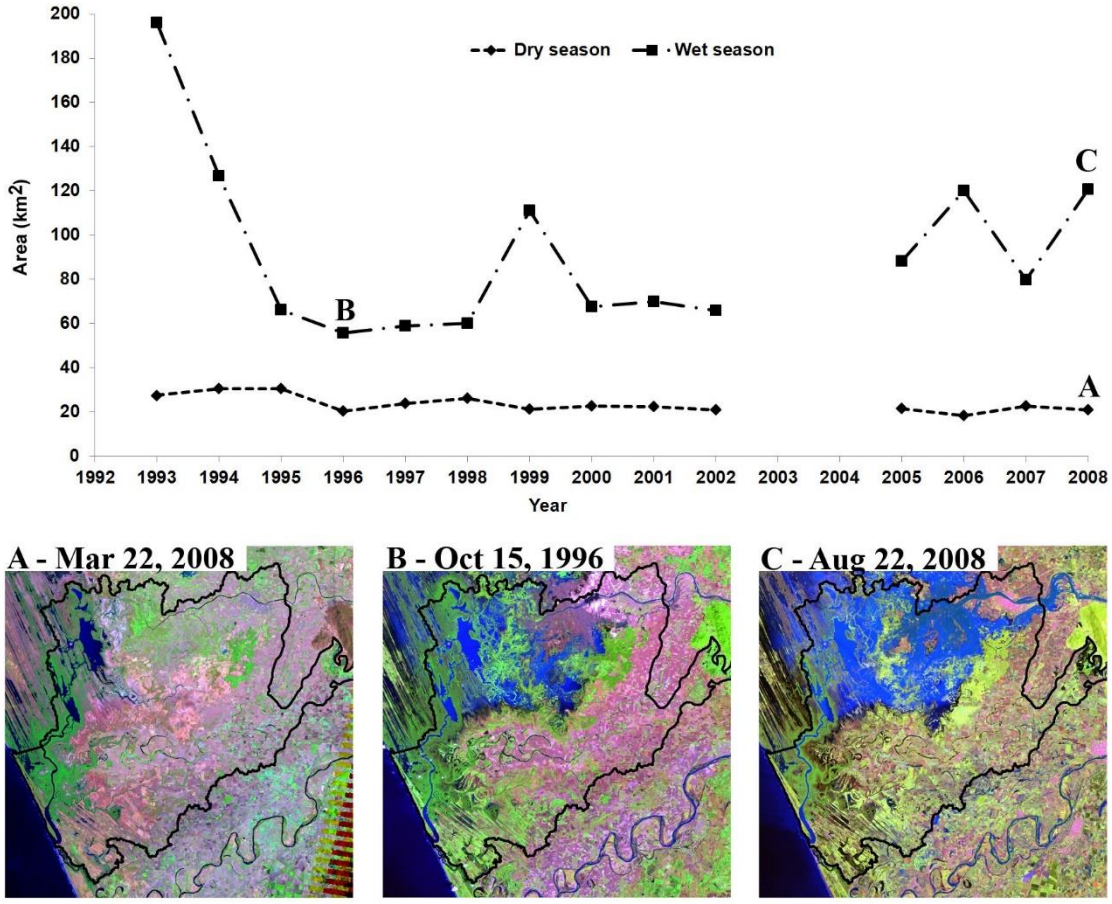

Figure 2. Inter-annual variation of aquatic surfaces in the study area. a) Dry season, 2008; b) regular rainy season, 1996; c) rainy season with extreme rainfall, 2008. Solid black lines inside the images represent the study area.

but are not solely responsible for the differences in flood extent.

A graphical representation of the flood spreading is shown in Figure 4, showing the intra-annual variability associated with the aforementioned R and Q variations. The flooding spatial pattern along the year, as detected by the imagery analysis, starts with the lowest levels at the dry season with around 25 km^2 in average, as previously estimated, when rainfall records were equal to 0 mm. The flood grows around Laguna Grande de Mexcaltitan system (to the northwest), expanding limits to the east up to altitudes around 10 m.a.s.l., south to the San Pedro River course, retreating to former distribution at the end of the year, when the dry season begins.

Floodwater distribution is mostly the same year by year, with variations attributable to differences in altitude, soil quality, R and Q values, besides the opportune satellite image recording to detect them, but the observed variations in extent during the dry season could be related to differences in the Q values, which do not depend on the rainfall recorded in the study area. In general, FE displayed its maximum values in August and September every year, increasing by up to four to five times the average extent observed in the dry season, similar to results obtained in the inter-annual analysis.

Although hydrological parameters are monthly represented (cumulative values) and water surface estimation is only representing a moment in the flood dynamics, there was a stronger positive correlation between R and FE ($r = 0.83$; $P < 0.01$). However, the maximum R values in the study area were not always synchronized with the largest inundated areas, making clear that overflow does not depend directly on the local rainfall rates nor the Q volume, as the highest record for this parameter was in September 2008 (2637.7×10^6 m^3), while the maximum FE was recorded the previous month in the same year.

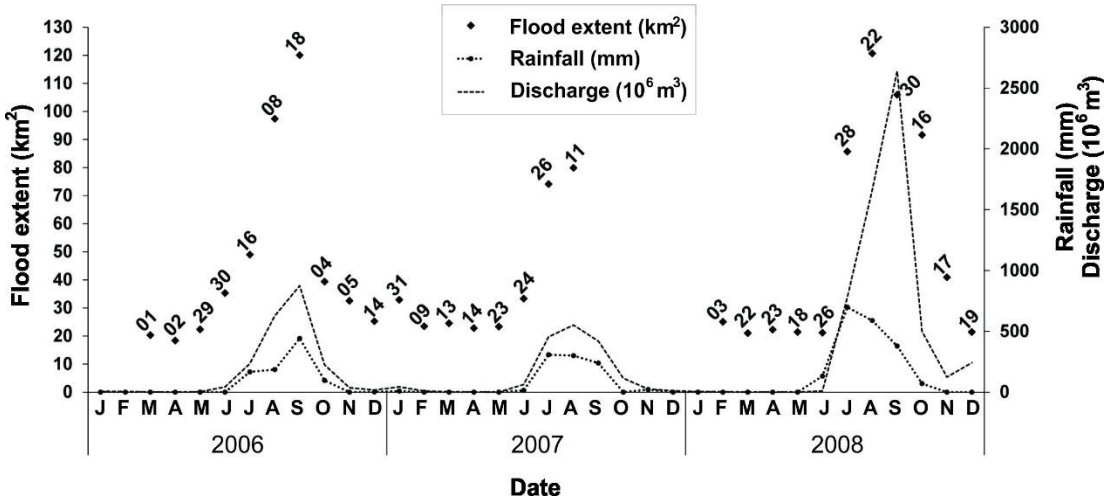

Figure 3. Flood extents estimated from Landsat image analyses; total rainfall and San Pedro River monthly discharge time series (2006-2008) in the study area. Figures above flood extent symbols represent day of the respective month.

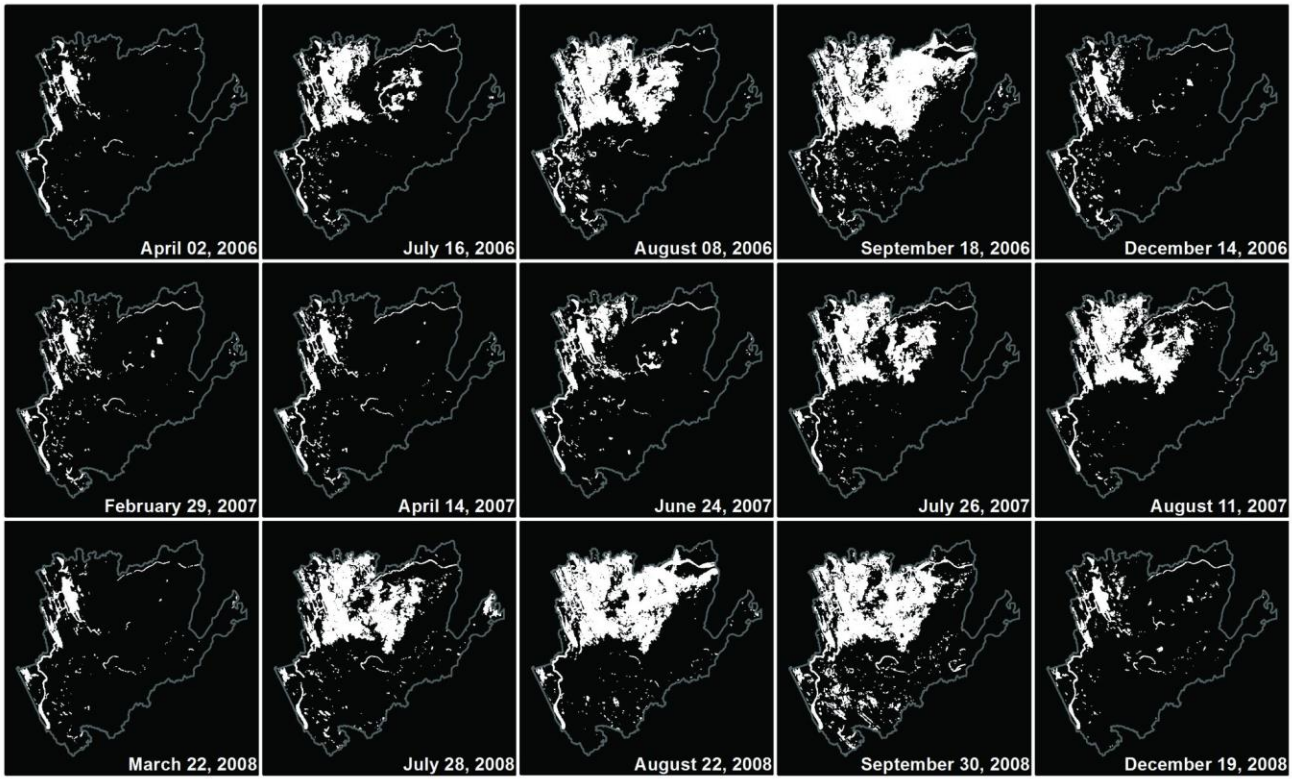

Figure 4. Temporal flood pattern in the San Pedro River lower basins as assessed by Landsat satellite imagery (2006-2008). Flooding in the study area is represented in white.

Despite those inconsistencies in temporal data, there is a clear pattern between the inundated area and Q values that involves limits to the flood extent. Considering that FE always maintains a minimum surface, approximately 25 km^2 corresponding to the perennial lagoons and estuaries, the relationship was fit to a particular case of an exponential model. This model is given by the three parameter single exponential rise to maximum type ($Y = y_0+a(1-b^X)$), with FE as the dependent variable. This model better explains and fits with the observed distribution pattern, and discards a linear model because a flattening in the curve occurs as discharge (Q) increases.

The dataset used consists of 29 pairs of Q (10^6 m^3) and FE (km^2) data, corresponding to the available imagery period included in this phase of the study. The observed data and the best fit model ($r^2 = 0.91$; $P < 0.01$) are shown in Figure 5. The final model is $FE = y_0 + a(1\text{-}0.9983^Q)$. The parameter y_0 is the offset from zero, corresponding to the dry season FE mean extent estimated over 21.3 km^2, a is the amplitude of the curve, equivalent to the maximum flood (99.5 km^2) and b is the dimensionless rate constant. Based on estimates of both y_0 and a, approximately 120 km^2 is expected as the maximum flood for the study area, which is consistent with the highest observed FE values in the dataset (September 2006 and August 2008).

DISCUSSION

Coastal wetlands are among the most threatened environments, deteriorated at worldwide level due in part to increasing population size (Mitsch & Gosselink, 2000; Kayastha *et al.,* 2012). Consequently, modifications of local hydrology and landscape are anticipated, including infrastructure to distribute hydrologic resources and to control potential inundation events (dams, reservoirs, channels), modifying flood patterns responsible for functional dynamics, maintenance, productivity and services that these ecosystems naturally provide to societies (Camacho *et al.,* 2014)

However, when knowledge of the dynamics of historical floods is limited, negative impacts may worsen with inadequately planned infrastructure. Besides changes in sediments and organic solids interchange and carbon intake rates alteration, biodiversity could reduce if flooding becomes permanent or if it is reduced, as inundated and dry phases are both required, even for species with mechanisms to survive periods of inundation (McKevlin *et al.,* 1998). Moreover, regular inundations are expected for the benefit of the local agriculture, being critical if intervals between large floods are lower than 10-20 years, depending on the crop (Nicholls & Wilson, 2001), but reducing productivity of soils if floods are eliminated.

Regarding the above scenarios, and recognizing that wetland maintenance depends on the availability of water, this study was carried out to gain knowledge of the flood pulse of the San Pedro River, but also contributes to conservation efforts of the Marismas Nacionales wetlands system, one of the largest and most complex coastal ecosystems in Mexico.

The San Pedro River is one of the main water and sediment sources for this system, which is currently threatened because of governmental plans to construct in the short term a hydroelectric dam (Las Cruces). The dam, which has been proposed to provide water throughout the year, has not proved its importance to regional development, and their impact on wetland ecosystem requirements has not been considered. As a first application of the exponential model developed in this study, we used the historic monthly average discharge (1944-2011) and the mean regulated discharge proposed for operating the Las Cruces hydroelectric dam (Contreras & Marceleño, 2013), with resulting estimates suggesting that most of the time (seven months each year) the study area will be flooded by approximately 7.0 km^2 more than average. During the rainy season, the mean flooding extent will be reduced by as much as 9.8 km^2, thereby reducing the flooded area by an average of 4.06 km^2.

In addition, results from the analysis of Landsat imagery, supported by ancillary data, reveal that even when flooding peaks are evident every few years, it is not possible to confirm a regular flooding pulse based on the available data series, which is less than 20 years, and although this approximation to the inter- and intra-annual flood dynamics could be useful for wetlands management purposes, there is not enough information to predict intense flooding as observed in 1993, having negative impacts on ecosystems and the local economy.

As above mentioned, extensive agriculture is the main economic activity in the region and it is particularly developed in the floodplain, exposed to periodic intra- and inter-annual floods, which depending on the flood magnitude and duration is positive or potentially negative for agricultural yields. Floods have been present historically and locals are aware of them, but negative impacts could potentially increase due to climate change effects (sea level rise and increase in the quantity and intensity of tropical storms), coupled with a growth of agriculture boundaries, particularly because floods do not follow a predictable pattern.

The flood pulsing phenomenon occurs recurrently in this river system and can be associated with runoff and upland rainfall patterns. It is not constrained by any man-made structure, thus allowing the exchange of materials and organisms among a mosaic of habitats. This plays a key role in determining the level of biological productivity and diversity in Marismas Nacionales (De la Lanza-Espino *et al.,* 2012). Flood pulsing is evident in the rainy season, particularly when tidal amplitude and freshwater input due to rainfall and groundwater recharge increases. However, due to the temporal resolution of Landsat imagery, differences in tide levels cannot be detected, creating a source of error. Due to lack of monitoring, additional data are needed to confirm the role of each hydrological parameter in the flood pulse patterns.

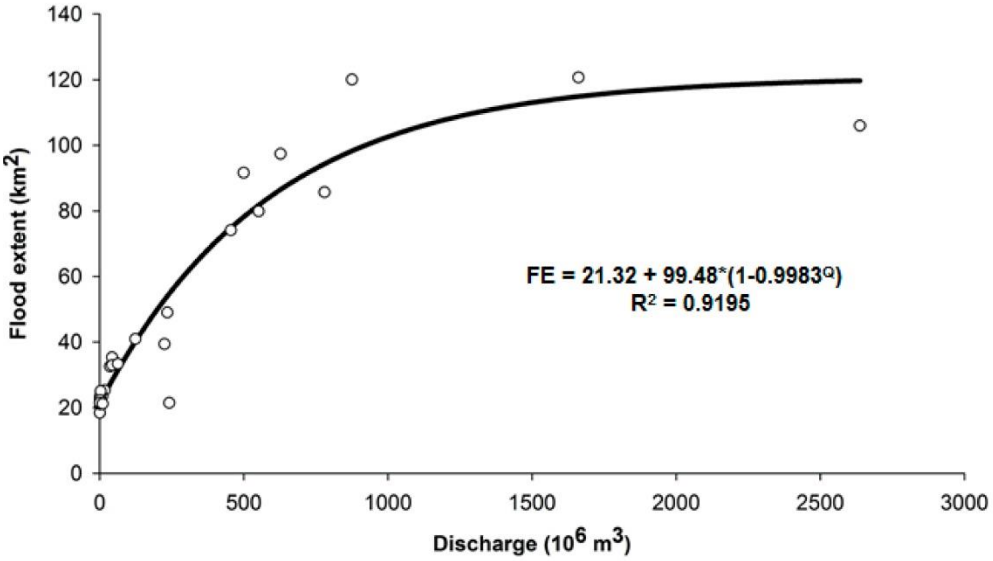

Figure 5. Flood extent *vs* total discharge in the study area (San Pedro River low basin) fitted to an exponential model.

Although several authors have demonstrated the value of multi-temporal images to evaluate wetland extent and condition in the Marismas Nacionales complex (Kovacs *et al.,* 2001; Berlanga-Robles & Ruiz-Luna, 2002, 2008; Hernández-Guzmán *et al.,* 2008; Kovacs *et al.,* 2008), little information exists on the relationship of the coastal ecosystems and flood pulses. The intra-annual flood pulse in the San Pedro River lower basin is characterized by a unimodal pattern with peaks in summer, similar to those reported for river deltas of the Okavango (Andersson *et al.,* 2006; Wolski *et al.,* 2006; Wolski & Murray-Hudson, 2006), the Mekong (Sakamoto *et al.,* 2007; Västilä *et al.,* 2010) and the Amazon (Alsdorf *et al.,* 2007; Martinez & Le Toan, 2007), where rainfall and runoff are the main drivers of flood extent. This pattern can vary based on the timing and extent of the rainy season, and occasionally by the influence of hurricanes and tropical storms. Additionally, the annual sea level cycle in many locations in the Mexican Pacific has its highest values in the summer (Zavala-Hidalgo *et al.,* 2010), increasing the flooding risk in that period.

Present findings suggest that every few years the water surface in the floodplain can reach its maximum area, approximately 120 km^2 or even more, part of which (approximately 25 km^2) is composed of perennial aquatic systems (lagoons, estuaries). Due to the limitations of the time series, it is not possible to detect any periodicity or to prove that extreme flooding is increasing in frequency. Based on geomorphology and runoff analyses in the same study region, Romo & Ortiz-Pérez (2001) propose that 2, 3-5, 50 and 100 year flood events will increase in severity, but with an accompanying decrease in the probability of occurrence.

According to present results, the largest flood was observed in 1993, as estimated via the analysis of a Landsat scene (September 13, 1993) (Fig. 2). This flood almost doubled the maximum estimated by our model, and its extent seemed to correspond with hurricane Lidia (September 8-14, 1993), which produced cumulative rainfall (3-day) from >30 to 245 mm, recorded in the stations located close to the study area (http://redesclim.org.mx/huracanes.php?h=Lidia1993). Previously, rainfall records >30 mm (3 day) were produced in the same area by hurricane Calvin (July 08, 1993), limiting infiltration ability in the area. A similar situation, with large floods, was described by Hudson & Colditz (2003) in the Panuco River (Gulf of Mexico), as a consequence of hurricane Gert (September 14-21, 1993), which also affected the study area; arriving there as tropical depression, after it crossed Mexico east to west.

Although the presence of tropical storms and hurricanes explain other flood episodes, there is not a direct relationship. Hurricanes Rosa (1994) and Kena (2002) also had negative effects on the Nayarit coastal ecosystems, particularly on mangroves (Kovacs *et al.,* 2001; Tovilla & Orihuela, 2004), but they had little influence on flooding and did not have rain volumes as high as those produced by hurricane Lidia. However, they did cause serious damage because of abrasive 230 km h^{-1} winds. In other cases, even when Landsat images were not available to match with meteorological events, it was possible to study the imagery analyzed with previous or subsequent records and again, hurricanes

and tropical storms are not necessarily a condition for flooding in the study area. Rainfall in the upper basin, and the consequent runoff produced, could be the main driver that explains situations such as the one observed in 2008.

Remote sensing is a practical way to obtain spatial information concerning the behavior of large dynamic systems such as the San Pedro River and our analysis of Landsat imagery provided an economical method for monitoring flood events in large fluvial systems over a relatively large time series, even when it is not possible to follow the temporal flood dynamics in detail. Present results are useful to answer questions concerning flood spreading, dynamics related with the maintenance of coastal wetlands and even flood risk prevention.

Although the spatial and radiometric resolution of the satellite images is sufficient to reliably evaluate flood extent, the temporal resolution is not adequate to provide data on flood dynamics. Monitoring of these flood pulses is a challenge because of their ephemeral nature, but this information is necessary not only for flood management planning purposes but also to predict the effects of further hydrological engineering works, such as the planned construction of Las Cruces hydroelectric dam. Developers must understand that if regional development depends on large infrastructure implementation, it is imperative to identify the biota adaptations to the local flood pulses and the possible impacts of modifying them due to dam construction, to minimize negative impacts by an appropriate management.

ACKNOWLEDGEMENTS

This research was supported by CONACYT and SEMARNAT (R. Hernández-Guzmán PhD research grant; FONSEC SEMARNAT 2002-C01-0112/A-1). We thank Inter-American Institute for Global Change Research for its financial support to the authors. Finally, we thank three anonymous reviewers for their so-called insights.

REFERENCES

Alsdorf, D., P. Bates, J. Melack, M. Wilson & T. Dunne. 2007. Spatial and temporal complexity of the Amazon flood measured from space. Geophys. Res. Lett., 34: 1-5.

Andersson, L., J. Wilk, M.C. Todd, D.A. Hughes, A. Earle, D. Kniveton, R. Layberry & H.H.G. Savenije. 2006. Impact of climate change and development scenarios on flow patterns in the Okavango River. J. Hydrol., 331: 43-57.

Benke, A.C., I. Chaubey, G.M. Ward & L. Dunn. 2000. Flood pulse dynamics of an unregulated river floodplain in the southeastern U.S. coastal plain. Ecology, 81: 2730-2741.

Berlanga-Robles, C.A. & A. Ruiz-Luna. 2002. Land use and mapping and change detection in the coastal zone of northwest Mexico using remote sensing techniques. J. Coast. Res., 18: 514-522.

Berlanga-Robles, C.A. & A. Ruiz-Luna. 2006. Evaluación de cambios del paisaje y sus efectos sobre humedales costeros en el sistema estuarino de San Blas, Nayarit, México, por medio de análisis de imágenes Landsat. Cienc. Mar., 32: 523-538.

Berlanga-Robles, C.A. & A. Ruiz-Luna. 2011. Integrating remote sensing techniques, geographical information systems (GIS), and stochastic models for monitoring land use and land cover (LULC) changes in the northern coastal region of Nayarit, Mexico. GISci. Remote Sens., 48: 245-263.

Berlanga-Robles, C.A., A. Ruiz-Luna & P. Trujillo-Batiz. 2008. Inventario de los humedales costeros del sistema lagunar Altata-Ensenada de Pabellón, Sinaloa, México a partir del análisis digital de imágenes de satélite Landsat TM del 2005. Rev. Invest. Mar., 29(1): 3-11.

Blanco, M. & M. Correa (eds.). 2011. Diagnóstico funcional de marismas nacionales. Universidad Autónoma de Nayarit - Comisión Nacional Forestal - DEFRA UK, Nayarit, Informe Final, 190 pp.

Camacho-Valdez, V., A. Ruiz-Luna, A. Ghermandi, C.A. Berlanga-Robles & P.A.L.D. Nunes. 2014. Effects of land use changes on the ecosystem service values of coastal wetlands. Environ. Manage., 54(4): 852-864.

Chormanski, J., T. Okruszko, S. Ignar, O. Batelaan, K.T. Rebel & M.J. Wassen. 2011. Flood mapping with remote sensing and hydrochemistry: a new method to distinguish the origin of flood water during floods. Ecol. Eng., 37: 1334-1349.

Contreras, R.S.H. & F.S.M.L. Marceleño. 2013. Manifestación de impacto ambiental modalidad regional (MIA-Rl) del Proyecto Hidroeléctrico (PH) Las Cruces, en el Estado de Nayarit. Comisión Federal de Electricidad/Universidad de Guadalajara/Universidad Autónoma de Nayarit, Informe Final, 1249 pp.

De la Lanza-Espino, G., J.L. Carbajal-Pérez, S.A. Salinas-Rodríguez & J.E. Barrios-Ordóñez. 2012. Medición del caudal ecológico del río Acaponeta, Nayarit, comparando distintos intervalos de tiempo. Invest. Geogr., 78: 62-74.

Frazier, P. & K. Page. 2009. A reach-scale remote sensing technique to relate wetland inundation to river flow. River Res. Appl., 25: 836-849.

Frazier, P., K. Page, J. Louis, S. Briggs & A.I. Robertson. 2003. Relating wetland inundation to river flow using Landsat TM data. Int. J. Remote Sens., 24: 3755-3770.

Hernández-Guzmán, R., A. Ruiz-Luna & C.A. Berlanga-Robles. 2008. Assessment of runoff response to landscape changes in the San Pedro subbasin (Nayarit, Mexico) using remote sensing data and GIS. J. Environ. Sci. Health. A, 43: 1471-1482.

Hudson, P.F. & R.R. Colditz. 2003. Flood delineation in a large and complex alluvial valley, lower Pánuco basin, Mexico. J. Hydrol., 280: 229-245.

Infante-Mata, D., P. Moreno-Casasola & C. Madero-Vega. 2012. Litterfall of tropical forested wetlands of Veracruz in the coastal floodplains of the Gulf of Mexico. Aquat. Bot., 98: 1-11.

Instituto Nacional de Estadística y Geografía (INEGI). 1999. Síntesis de información geográfica del estado de Nayarit. Instituto Nacional de Estadística y Geografía (INEGI), México, 140 pp.

Junk, W.J. & K.M. Wantzen. 2004. The flood pulse concept: new aspects, approaches and applications - an update. 2nd International Symposiun of Management of Large Rivers for Fisheries. FAO Regional Office for Asia and the Pacific, RAP Publication 2004/16, Bangkok, pp. 117-149.

Junk, W.J., P.B. Bayley & R.E. Sparks. 1989. The flood pulse concept in river-floodplain systems. In: D.P. Dodge (ed.). Proceedings of the International Large River Symposium. Can. Spec. Publ. Fish. Aquat. Sci., 106: 110-127.

Kayastha, N., V. Thomas, J. Galbraith & A. Banskota. 2012. Monitoring wetland change using inter-annual landsat time-series data. Wetlands, 32: 1149-1162.

Knight, A.E., D.R. Tindall & B.A. Wilson. 2009. A multitemporal multiple density slice method for wetland mapping across the state of Queensland, Australia. Int. J. Remote Sens., 30(13): 3365-3392

Kovacs, J.M., M. Blanco-Correa & F. Flores-Verdugo. 2001. A logistic regression model of hurricane impacts in a mangrove forest of the Mexican Pacific. J. Coast. Res., 17: 30-37.

Kovacs, J.M., C. Zhang & F.J. Flores-Verdugo. 2008. Mapping the condition of mangroves of the Mexican Pacific using C-band ENVISAT ASAR and Landsat optical data. Cienc. Mar., 34: 407-418.

McKevlin, M.R., D.D. Hook & A.A. Rozelle. 1998. Adaptations of plants to flooding and soil water-logging. In: M.G. Messina & W.H. Conner (eds.). Southern forested wetlands: ecology and management. CRC Press, Boca Raton, pp. 173-203.

Martinez, J.M. & T. Le Toan. 2007. Mapping of flood dynamics and spatial distribution of vegetation in the Amazon floodplain using multitemporal SAR data. Remote Sens. Environ., 108: 209-223.

Matgen, P., A. El Idrissi, J.B. Henry, N. Tholey, L. Hoffmann, P. de Fraipont & L. Pfister. 2006. Patterns of remotely sensed floodplain saturation and its use in runoff predictions. Hydrol. Processes, 20: 1805-1825.

Middleton, B.A. 2002. The flood pulse concept in wetland restoration. In: B.A. Middleton (ed.). Flood pulsing in wetlands: restoring the natural hydrological balance. Wiley, New York, pp. 1-10.

Mitsch, W.J. & J.G. Gosselink. 2000. Wetlands. John Wiley & Sons, New York, 920 pp.

Nicholls, R.J. & T. Wilson. 2001. Integrated impacts on coastal areas and river flooding. In: I.P. Holman & P.J. Loveland (eds.). REGIS-Regional climate change impact and response studies in East Anglia and North West England, UKCIP Technical Report. Soil Survey and Land Research Centre, London, pp. 54-103.

Ortiz-Pérez, M.A. & A. Pérez-Vega. 1999. Evidencia documental de los cambios de la línea de costa por sedimentación rápida en la bahía de Matanchén, Nayarit, México. Invest. Geogr., 40: 58-70.

Pricope, N.G. 2012. Variable-source flood pulsing in a semi-arid transboundary watershed: the Chobe River, Botswana and Namibia. Environ. Monit. Assess., 185: 1883-1906.

Qi, S., D.G. Brown, Q. Tian, L. Jiang, T. Zhao & K.M. Bergen. 2009. Inundation extent and flood frequency mapping using Landsat imagery and Digital Elevation Models. GISci. Remote Sens., 46: 101-127.

Rebelo, L.M., G.B. Senay & M.P. McCartney. 2012. Flood pulsing in the Sudd wetland: analysis of seasonal variations in inundation and evaporation in South Sudan. Earth Interact., 16: 1-19.

Richards, J.A. & X. Jia. 1999. Remote sensing digital image analysis. Springer, New York, 363 pp.

Romo, M.L. & M.A. Ortiz-Pérez. 2001. Riesgo de inundación en la llanura fluvial del curso bajo del río San Pedro, Nayarit. Invest. Geogr., 45: 7-23.

Sakamoto, T., N.V. Nguyen, A. Kotera, H. Ohno, N. Ishitsuka & M. Yokozawa. 2007. Detecting temporal changes in the extent of annual flooding within the Cambodia and the Vietnamese Mekong Delta from MODIS time-series imagery. Remote Sens. Environ., 109: 295-313. doi:10.1016/j.rse.2007.01.011.

Smith, L.C., B.L. Isacks, R.R. Forster, A.L. Bloom & I. Preuss. 1995. Estimation of discharge from braided glacial rivers using ERS 1 synthetic aperture radar: first results. Water Resour. Res., 31: 1325-1329.

Stillman, J.H. & F.H. Barnwell. 2004. Relationship of daily and circatidal activity rhythms of the fiddler crab, *Uca princeps*, to the harmonic structure of semidiurnal and mixed tides. Mar. Biol., 144: 473-482.

Tovilla, H.C. & D.E.B. Orihuela. 2004. Impacto del huracán Rosa sobre los bosques de manglar de la costa de Nayarit, México. Madera Bosques, 10: 63-75.

Townshend, J.R.G. & C.O. Justice. 1990. The spatial variation of vegetation changes at very coarse scales. Int. J. Remote Sens., 11(1): 149-157.

Valdez, H.J.I. 2004. Manejo forestal de un manglar al sur de Marismas Nacionales, Nayarit. Madera Bosques, 2: 93-104.

Västilä, K., M. Kummu, C. Sangmanee & S. Chinvanno. 2010. Modelling climate change impacts on the flood pulse in the Lower Mekong floodplains. J. Water Climate Change., 1: 67-86.

Received: 18 December 2014; Accepted: 14 January 2016

Wolski, P. & M. Murray-Hudson. 2006. Flooding dynamics in a large low-gradient alluvial fan, the Okavango Delta, Botswana, from analysis and interpretation of a 30-year hydrometric record. Hydrol. Earth Syst. Sci., 2: 127-137.

Wolski, P., H.H.G. Savenije, M. Murray-Hudson & T. Gumbricht. 2006. Modelling of the flooding in the Okavango Delta, Botswana, using a hybrid reservoir-GIS model. J. Hydrol., 331: 58-72.

Zavala-Hidalgo, J., R. de Buen, K.R. Romero-Centeno & F. Hernández-Maguey. 2010. Tendencias del nivel del mar en las costas mexicanas. In: V.A. Botello, S. Villanueva-Fragoso, J. Gutiérrez & J.L. Rojas-Galaviz (eds.). Vulnerabilidad de las zonas costeras mexicanas ante el cambio climático, SEMARNAT-INE-UNAM-ICMYL, Universidad Autónoma de Campeche, Campeche, pp. 249-268.